Reactive Oxygen Species Regulate Angiogenesis and Tumor Growth through Vascular Endothelial Growth Factor

Chang Xia,[1] Qiao Meng,[1] Ling-Zhi Liu,[1] Yongyut Rojanasakul,[2] Xin-Ru Wang,[3] and Bing-Hua Jiang[1]

[1]Mary Babb Randolph Cancer Center, and Departments of Microbiology, Immunology and Cell Biology and [2]Pharmaceutical Sciences, West Virginia University, Morgantown, West Virginia; and [3]Lab of Reproductive Medicine, Cancer Center, Nanjing Medical University, Nanjing, Jiangsu, China

Abstract

Reactive oxygen species (ROS) are associated with multiple cellular functions such as cell proliferation, differentiation, and apoptosis. However, the direct roles of endogenous ROS production still remain to be elucidated. In this study, we found that high levels of ROS were spontaneously produced by ovarian and prostate cancer cells. This elevated ROS production was inhibited by NADPH oxidase inhibitor diphenylene iodonium (DPI) and mitochondria electron chain inhibitor rotenone in the cells. To further analyze the source of ROS production, we found that ovarian cancer cells have much higher expression of NOX4 NADPH oxidase, and that specific inhibition of NADPH oxidase subunit $p47^{phox}$ diminished ROS production. To analyze the functional relevance of ROS production, we showed that ROS regulated hypoxia-inducible factor 1 (HIF-1) and vascular endothelial growth factor (VEGF) expression in ovarian cancer cells. Elevated levels of endogenous ROS were required for inducing angiogenesis and tumor growth. NOX4 knockdown in ovarian cancer cells decreased the levels of VEGF and HIF-1α and tumor angiogenesis. This study suggests a new mechanism of higher ROS production in ovarian cancer cells and provides strong evidence that endogenous ROS play an important role for cancer cells to induce angiogenesis and tumor growth. This information may be useful to understand the new mechanism of cancer cells in inducing tumorigenesis and to develop new therapeutic strategy by targeting ROS signaling in human cancer in the future. [Cancer Res 2007;67(22):10823–30]

Introduction

Reactive oxygen species (ROS) are naturally produced by cells through aerobic metabolism, and high levels of ROS in the cells are associated with many diseases including cancer (1, 2). Several lines of evidence indicate that ROS may be involved in human carcinogenesis: (*a*) some growth factors such as epidermal growth factor (EGF), insulin, and angiopoietin-1 increase ROS production in the cells for regulating cell migration and proliferation (3–6); (*b*) natural antioxidants can inhibit cancer cell proliferation and tumor growth (7–10); (*c*) high levels of ROS are observed in some cancer cells, which may induce DNA damage leading to genomic instability and tumor initiation (11, 12); and (*d*) ROS induce the activation of mitogen-activated protein (MAP) kinase, nuclear factor κB (NF-κB), and activator protein 1, which are known to be associated with cancer development (13–15). However, under certain conditions, ROS increase proapoptotic molecules such as p53 and p38 MAP kinase and induce cellular apoptosis (16, 17). The direct role of ROS in tumor growth and angiogenesis remains to be defined. Angiogenesis is important for tumor development and growth (18). The vascular endothelial growth factor (VEGF) is a major angiogenesis inducer and is regulated at transcriptional level by hypoxia-inducible factor 1 (HIF-1) in response to hypoxia (19, 20). HIF-1 is composed of HIF-1α and HIF-1β subunits (20, 21). In this study, we found that ovarian cancer cells had elevated levels of ROS production; thus, we further analyzed (*a*) what the source and mechanism of endogenous ROS production in ovarian cancer cells were; (*b*) whether endogenous ROS production regulated HIF-1 and VEGF expression; (*c*) whether ROS generation in the cells was required for inducing angiogenesis and tumor growth *in vivo*; and (*d*) whether ROS regulated angiogenesis and tumor growth through HIF-1α and VEGF expression. This work would provide the direct evidence of the endogenous ROS in regulating tumor growth and angiogenesis *in vivo* and a new sight in the underlying mechanisms.

Materials and Methods

Reagents and cell culture. The human ovarian cancer cells OVCAR-3 and A2780 and immortalized ovarian surface epithelial cells IOSE 397 and IOSE 386 were maintained in RPMI 1640 (Invitrogen) supplemented with 10% fetal bovine serum (FBS), 2 mmol/L L-glutamine, 100 units/mL penicillin, and 100 μg/mL streptomycin and cultured at 37°C in a 5% CO_2 incubator. Trypsin (0.25%)/EDTA solution was used to detach the cells from the culture flask. Antibodies against HIF-1α and HIF-1β were from BD Biosciences. Antibodies against VEGF for ELISA and immunohistochemistry were purchased from R&D System and Santa Cruz Biotechnology, respectively. Diphenylene iodonium (DPI) and rotenone were from Sigma. 2′,7′-Dichlorofluorescein diacetate (CM_2-DCFHDA) was from Molecular Probes.

Intracellular H_2O_2 staining. Ovarian cancer cells or immortalized ovarian surface epithelial cells were seeded in six-well plate at density of 1×10^5 cells per well on a coverslip overnight. The cells were stained with CM_2-DCFHDA (5 μmol/L) for 15 min at 37°C, then washed with 1× PBS thrice, and fixed with 10% formaldehyde. Images were captured with a Zeiss Axiovert 100 TV microscope with a 40 × 1.4 objective lens with a laser scanning confocal attachment (LSM 510; Zeiss). Quantification of immunofluorescence intensity was done using the confocal microscope with 480-nm excitation and 540-nm emission settings.

Immunoblotting analysis. The total cellular protein extracts were prepared in radioimmunoprecipitation assay buffer (RIPA) and separated by 7% SDS-PAGE. Membranes were blocked with 5% nonfat dry milk for 2 h and incubated with primary antibodies. Protein bands were detected by incubation with horseradish peroxidase–conjugated antibodies (Perkin-Elmer Life Sciences) and visualized with enhanced chemiluminescence reagent.

Note: Supplementary data for this article are available at Cancer Research Online (http://cancerres.aacrjournals.org/).

C. Xia, Q. Meng, and L.Z. Liu contributed equally to this work.

Requests for reprints: Bing-Hua Jiang, Mary Babb Randolph Cancer Center, and Department of Microbiology, Immunology and Cell Biology, West Virginia University, 1801 Health Sciences South, Morgantown, WV 26506. Phone: 304-293-5949; Fax: 304-293-4667; E-mail: bhjiang@hsc.wvu.edu.

doi:10.1158/0008-5472.CAN-07-0783

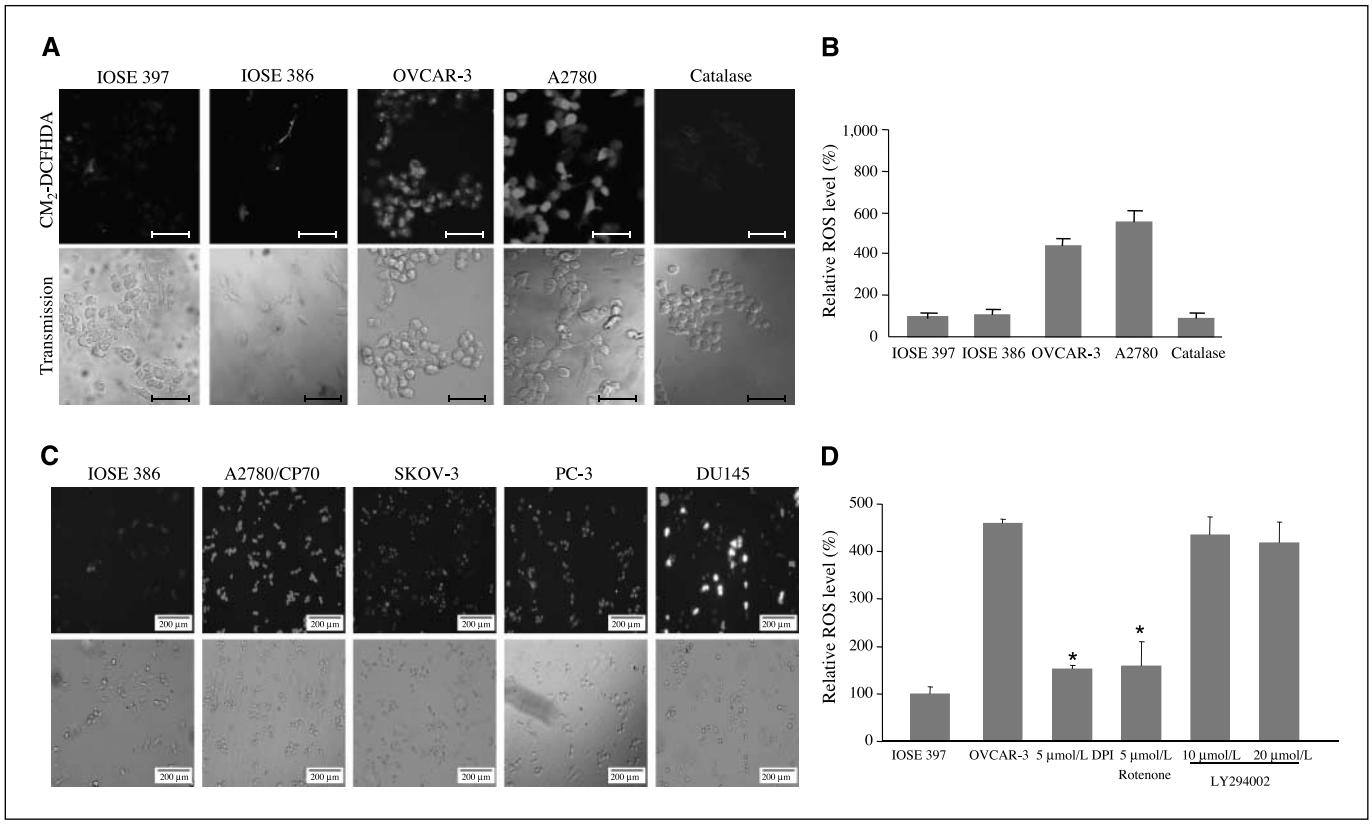

Figure 1. Ovarian cancer cell lines generate higher levels of endogenous ROS. *A,* ovarian cancer cells OVCAR-3 and A2780 and immortalized ovarian surface epithelial cells IOSE 386 and IOSE 397 were seeded onto a glass coverslip in the six-well plate at 1×10^5 cells per well for 24 h. CM_2-DCFHDA (5 μmol/L) was added into the cell culture medium and incubated for 30 min. For the catalase treatment, catalase (750 units/mL) was added to A2780 cells 30 min before the addition of CM_2-DCFHDA. The cells were washed thrice with 1× PBS and fixed with 10% buffered formalin. The representative images were captured with a confocal fluorescence microscope (at excitation wavelength, 485 nm; emission wavelength, 530 nm). *Bar*, 50 μm. *B,* the mean value of DCF fluorescence intensity was obtained from 10,000 cells at 485 nm excitation and 540 nm emission settings using a flow cytometer (Becton Dickinson FACSort). *C,* IOSE 386, A2780/CP70, SKOV-3, PC-3, and DU145 were seeded onto a glass coverslip in the six-well plate at 1×10^5 cells per well for 24 h. CM_2-DCFHDA (5 μmol/L) was added into the cell culture medium and incubated for 30 min. The cells were washed thrice with 1× PBS and fixed with 10% buffered formalin. The representative fluorescence (*top*) and phase contrast (*bottom*) images were captured with a confocal fluorescence microscope. *Bar*, 200 μm. *D,* OVCAR-3 cells were treated with solvent, 5 μmol/L DPI, 5 μmol/L rotenone, 10 or 20 μmol/L LY294002 for 30 min and then stained with 5 μmol/L CM_2-DCFHDA for 15 min. The relative fluorescence intensity was analyzed by flow cytometry and normalized to that of IOSE 397 cells. *, $P < 0.01$, significant difference when the value of treatment was compared with that of the control.

Transient transfection. Small interfering RNA (siRNA) duplex oligonucleotides targeting human $p47^{phox}$ and NOX4 were purchased from Dharmacon. OVCAR-3 cells were cultured to 60% to 70% confluency in 35-mm dishes and transfected with $p47^{phox}$ siRNA or NOX4 siRNA using X-tremeGENE siRNA transfecting reagent (Roche Applied Science) in serum-free OPTIMEM according to the manufacturer's instruction. The cells were switched to fresh medium (1 mL) containing 10% FBS 3 h after the transfection and cultured for 24 to 72 h. The $p47^{phox}$ protein expression in the cells was analyzed by immunoblotting, and ROS levels in the cells were analyzed by DCFHDA staining. The cells transfected with NOX4 siRNA were used for analyzing VEGF and HIF-1 expression and angiogenesis response.

ELISA. Capture ELISA was done using a human VEGF ELISA kit according to the manufacturer's instruction (R&D Systems). Optical densities were read at 405 nm, and the rate of VEGF secretion was calculated as we previously described (22).

Semiquantitative reverse transcription-PCR. Total RNAs were isolated with TRIzol reagent (Life Technologies). First-strand cDNAs were synthesized using total RNAs, avian myeloblastosis virus (AMV) reverse transcriptase, and an oligo(dT) primer (Promega). Primers used for PCR amplification were as follows: VEGF sense primer, 5′-TCGGGCCTCCGAAACCATGA-3′; VEGF antisense primer, 5′-CCTGGTGAGAGATCTGGTTC-3′; glyceraldehyde-3-phosphate dehydrogenase (GAPDH) sense: 5′-CCACCCATGGCAAATTCCATGGCA-3′; GAPDH antisense: 5′-TCTAGACGGCAGGTCAGGTCCACC-3′; NOX4 sense: 5′-CTCAGCGGAATCAATCAGCTGTG-3′; NOX4 antisense: 5′-AGAGGAACACGACAATCAGCCTTAG-3′. Reverse transcription-PCR (RT-PCR) reaction was done for 30 cycles with each cycle for 1 min at 94°C, 1 min at 55°C, and 1 min at 72°C. Quantification of PCR product was done by electrophoresis.

Luciferase assay. OVCAR-3 cells were cultured in 12-well plates and transiently transfected with human VEGF reporter (1 μg) and β-galactosidase (0.2 μg) plasmids. The cells were cultured for 48 h after the transfection, and relative luciferase activities were analyzed as we described (22).

Tumor-induced angiogenesis on chicken chorioallantoic membrane. White Leghorn fertilized chicken eggs were incubated at 37°C under constant humidity. To investigate the effect of ROS inhibitors on tumor-induced angiogenesis, OVCAR-3 cells (1×10^6) with or without DPI (500 nmol/L) or rotenone (200 nmol/L) treatment were mixed at 1:1 ratio with Matrigel and implanted onto the chorioallantoic membranes (CAM) at day 9. Tumor angiogenesis was analyzed 4 days after the implantation, and tumor growth was analyzed 9 days after the implantation. Similarly, OVCAR-3 cells were infected with 10 multiplicity of infection (MOI) adenovirus carrying green fluorescent protein, catalase, or GPx. the cells were used to perform angiogenesis and tumor growth assay. The blood vessel branches on the CAM were counted by two observers in a double-blind manner. The representative tumors were photographed.

Immunohistochemistry staining. Tissues harvested from the CAM were fixed in 10% formaldehyde overnight and then embedded in paraffin.

Sections (5 μm) were collected on positively charged slides and deparaffinized in the following order: in xyline for 5 min, 100% alcohol for 5 min, 95% alcohol for 3 min, 70% alcohol for 3 min, and then rinsed thrice in deionized water. The slides were then steamed with antigen retrieval buffer [10 mmol/L citrate (pH 8.0)] for 10 min, cooled to room temperature for 20 min, and then rinsed thrice in deionized water. The slides were incubated with 5% goat serum at room temperature for 1 h and then stained with antibodies against VEGF or HIF-1α overnight at 4°C, followed by incubation with horseradish peroxidase–conjugated secondary antibodies for 1 h at room temperature. Between each step, the sections were washed thrice with PBS buffer.

Statistical analysis. The data were analyzed using ANOVA by SPSS statistics software package. All the results are expressed as mean ± SE, and the difference was considered significant at $P < 0.05$.

Results

Spontaneous ROS production in ovarian and prostate cancer cells. We used intracellular DCFHDA staining method to measure the endogenous ROS levels in the cells and found that the ROS levels in both OVCAR-3 and A2780 cells were 5- and 6-fold higher, respectively, than those in immortalized ovarian epithelial cells IOSE 397 and IOSE 386 (Fig. 1*A* and *B*). The fluorescent signal was completely inhibited by the addition of catalase to indicate the specificity of ROS staining. To further test the ROS levels in other cancer cells, ovarian cancer cell lines A2780/CP70, SKOV-3, and prostate cancer cells PC-3 and DU145 were used. As shown in Fig. 1*C*, the ROS levels in these four cell lines were much higher than that in IOSE 386 cells, indicating that ROS were also spontaneously produced in other ovarian and prostate cancer cell lines. The endogenous ROS production was inhibited by DPI, NADPH-dependent oxidase inhibitor, and rotenone, the mitochondria complex I inhibitor (Fig. 1*D*). Phosphoinositide-3-kinase (PI3K) inhibitor LY294002 did not inhibit the ROS generation. This result suggests that NADPH oxidase and the mitochondria respiratory chain are required for inducing ROS production in the cells.

Role of NADPH oxidase in regulating ROS production in ovarian cancer cells. The NADPH oxidase complex includes a catalytic subunit gp91^{phox} and regulatory subunits such as p47^{phox}, p67^{phox}, and Rac. The homologues of gp91^{phox} (also known as NOX2) are called NOX family members. To test the expression of NOX isoforms in ovarian cancer cells, the mRNA levels of NADPH oxidase isoforms were analyzed in OVCAR-3 and A2780 cells. As shown in Fig. 2*A*, NOX4 mRNA levels were much higher in ovarian cancer cells than those in immortalized normal ovarian epithelial cells. NOX1, NOX3, and NOX5 mRNA levels were not detectable in the ovarian cancer cells; and NOX2 mRNA level was not increased in the cells (data not shown). This result indicates that NOX4 overexpression may be responsible for higher NADPH activity to increase ROS production in the cells. The expression of NOX4 was significantly inhibited by the treatment of SB431542, the inhibitor of transforming growth factor-β1 (TGF-β1), and pyrrolidine dithiocarbamate (PDTC), a chemical inhibitor of NF-κB, indicating that the activation of TGF-β1 and NF-κB was involved in regulating NOX4 expression (Fig. 2*B*). To further test whether NADPH activity was required for increasing ROS levels in the ovarian cancer cells, we inhibited p47^{phox} expression, a regulatory subunit of NADPH oxidase, which is required for NADPH oxidase activity (23–25). The protein levels of p47^{phox} were markedly reduced by p47^{phox} siRNA as compared with the cells with mock transfection (Fig. 2*C*), indicating that p47^{phox} siRNA was sufficient to inhibit endogenous p47^{phox} expression. The transfection of p47^{phox} siRNA significantly diminished the endogenous ROS production (Fig. 2*D* and Supplementary Fig. S1). This result showed that specific inhibition of NADPH oxidase subunit decreased ROS production in the ovarian cancer cells, further confirming that NADPH oxidase is required for ROS generation in the cells.

Endogenous ROS regulated HIF-1α, but not HIF-1β expression. HIF-1α is induced by hypoxia in OVCAR-3 cells (Supplementary Fig. S2). To test whether endogenous ROS levels affect HIF-1α expression, OVCAR-3 cells were treated with DPI and rotenone. The treatment of both inhibitors decreased the expression of HIF-1α in a dose-dependent manner, but did not affect HIF-1β expression (Fig. 3*A*). To identify what species of ROS were required for regulating HIF-1α expression, we found that O_2^- scavenger superoxide dismutase treatment increased the levels of HIF-1α expression, H_2O_2 scavenger catalase inhibited HIF-1α expression in a dose-dependent manner, and OH^- scavenger sodium formate did not affect HIF-1α expression (Fig. 3*A*). This result showed that ROS regulated HIF-1α expression in the cells specifically through H_2O_2, but not O_2^- and OH^- levels. To test whether increased H_2O_2 levels were sufficient to induce HIF-1α expression, OVCAR-3 cells were exposed to 100 μmol/L H_2O_2. H_2O_2 treatment greatly increased HIF-1α expression, and HIF-1α expression gradually increased up to 6 h, whereas the HIF-1β level was not changed (data not shown). This result showed that H_2O_2 is sufficient to induce HIF-1α expression in the cells.

ROS production regulated VEGF transcriptional activation. To test whether ROS affected VEGF expression, OVCAR-3 cells were

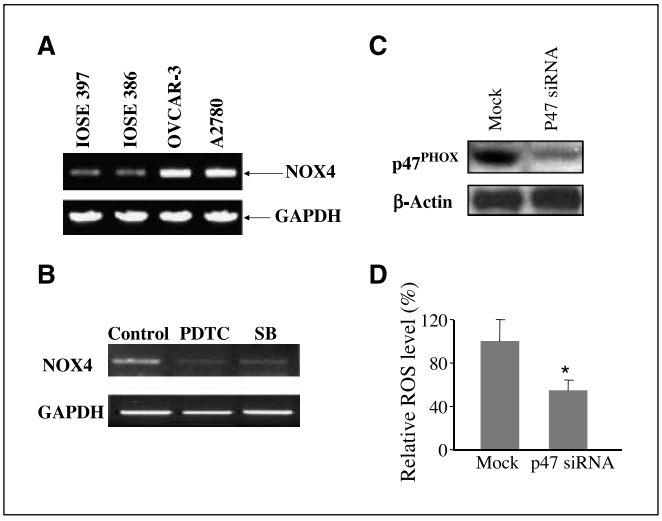

Figure 2. NADPH oxidase regulated ROS production in ovarian cancer cells. *A,* analysis of NOX family homologue expression in ovarian cancer cells and ovarian surface epithelial cells. Total RNAs were prepared using the TRIzol reagent, and RT-PCR was done using PCR primers specific for human NOX4 and GAPDH to test NOX4 levels in OVCAR-3, A2780, IOSE 386, and IOSE 397 cells. The PCR products of NOX4 and GAPDH are 300 and 550 bp, respectively. *B,* OVCAR-3 cells were treated with solvent, NF-κB inhibitor PDTC, and TGF-β1 inhibitor SB 431542 for 24 h. Then, total RNAs were extracted and analyzed for the mRNA levels of NOX4 and GAPDH by RT-PCR. *C,* OVCAR-3 cells were transfected with 20 nmol/L p47^{phox} siRNA using X-tremeGENE siRNA transfecting reagent. Total protein lysates were extracted and subjected to immunoblotting using antibodies against p47^{phox} and β-actin. *D,* OVCAR-3 cells were transfected with 20 nmol/L p47^{phox} siRNA using X-tremeGENE siRNA transfecting reagent. The cells were allowed to recover for 24 h and then treated with 5 μmol/L CM_2-DCFHDA for 15 min at 37°C. Fluorescence images were photographed by confocal microscope and quantified from 10 fields. *, $P < 0.01$, significant difference when the value of treatment was compared with that of the control.

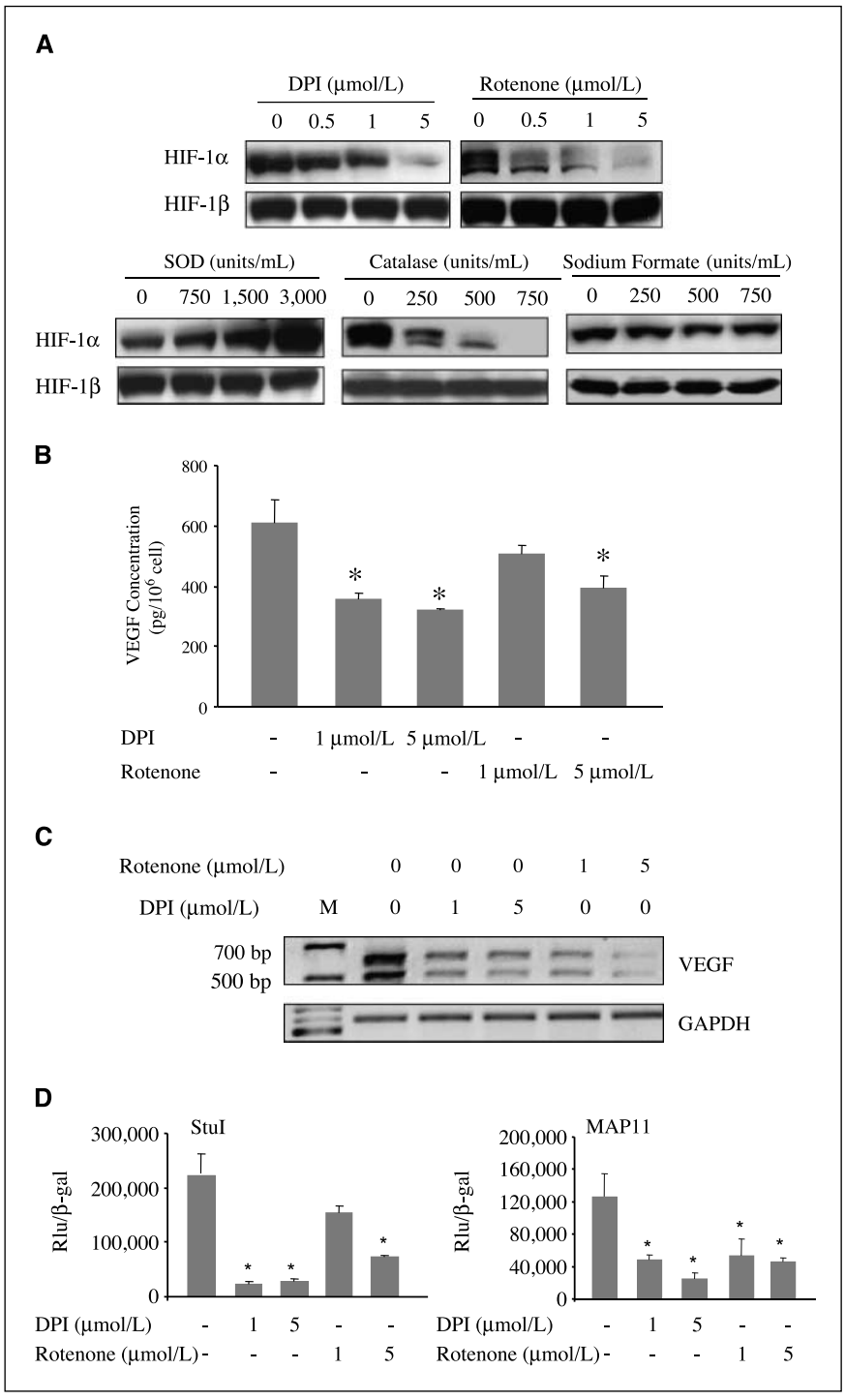

Figure 3. ROS regulated HIF-1α protein expression in ovarian cancer cells, and ROS inhibitors decreased VEGF expression and transcriptional activation. *A,* OVCAR-3 cells were treated with DPI (*top, left*), rotenone (*top, right*) for 4 h at the indicated concentrations. Total cellular lysates were subjected to immunoblotting analysis using antibodies against HIF-1α and HIF-1β (*top*). OVCAR-3 cells were treated with SOD (*bottom, left*), catalase (*bottom, middle*), and sodium formate (*bottom, right*) for 4 h at the indicated concentrations. The cellular lysates were subjected to immunoblotting analysis using antibodies against HIF-1α and HIF-1β (*bottom*). *B,* OVCAR-3 cells were seeded into 12-well plates and cultured to 90% confluence in complete medium. The cells were changed to fresh medium and treated with DPI or rotenone at indicated concentrations for 16 h. Then, 100 μL supernatants were used to analyze VEGF protein levels by ELISA. Data are presented as picograms of VEGF protein per 10^6 cells from six replicate experiments. *, $P < 0.05$, significant difference when the value of treatment was compared with that of the control. *C,* analysis of VEGF mRNA expression by semiquantitative RT-PCR. OVCAR-3 cells were treated with DPI or rotenone for 12 h at indicated concentrations. Total RNAs were extracted using TRIzol reagent, and the first-strand cDNAs were synthesized from 1 μg of total RNAs using AMV reverse transcriptase. Quantitation of the PCR products after 30 cycles was done by electrophoresis on 2% agarose gels and ethidium bromide staining. *D,* OVAR-3 cells were seeded in 12-well plates at 40% to 50% confluence the day before transfection. Cells were then transiently transfected with 0.5 μg VEGF promoter reporter pGL-Stu1 (*left*), or pMAP11wt (*right*) and 0.15 μg pCMV-β-galactosidase. After overnight recovery, the cells were treated with DPI or rotenone at indicated concentrations for 12 h. The relative luciferase activities were analyzed as described above. Data were mean ± SE of relative luciferase activities from three independent experiments. Each experiment was done with triplicate wells. *, $P < 0.05$, significant difference when the value of treatment was compared with that of the control.

treated with DPI and rotenone. As showed in Fig. 3*B*, VEGF protein expression in the cells was significantly inhibited by the treatment of DPI and rotenone. To further analyze the mechanism of ROS in regulating VEGF expression, we studied the effect of ROS inhibitors on VEGF mRNA expression and found that DPI and rotenone treatment significantly decreased VEGF mRNA steady level (Fig. 3*C*). As a control, GAPDH mRNA level was not affected by the ROS inhibitors. It is possible that ROS regulate VEGF mRNA expression at the transcriptional level through HIF-1 expression. To examine the effect of ROS production in VEGF transcriptional activation, the cells were transfected with a full-length human VEGF promoter. Treatment of DPI and rotenone greatly inhibited the VEGF reporter activity (Fig. 3*D*). This result suggests that ROS are required for VEGF transcriptional activation. To analyze whether it is mediated by HIF-1, a VEGF reporter containing only 46 bp functional promoter with the HIF-1 binding site was used. Similarly, addition of DPI and rotenone decreased the reporter activity (Fig. 3*D*). These data suggest that ROS regulate VEGF transcriptional activation through HIF-1α expression.

ROS regulated tumor-induced angiogenesis and tumor growth through HIF-1 and VEGF expression *in vivo*. To determine whether ROS are involved in tumor-induced angiogenesis *in vivo*, we employed the chicken CAM assay. OVCAR-3 cells were trapped in growth factor–free Matrigel without or with DPI or rotenone and implanted to the CAM. The treatment of ROS inhibitors decreased tumor-induced angiogenesis 4 days after the treatment (Fig. 4*A*). DPI and rotenone treatment decreased angiogenesis by 60% and 40%, respectively (Fig. 4*B*). The tumor mass was not much different at day 4 (data not showed). To further assess the role of ROS in tumor growth, we studied the tumor growth in the presence or absence of DPI and rotenone 9 days after the implantation. Tumor growth was suppressed by DPI and rotenone with 40% and 30% weight reduction, respectively (Fig. 4*C* and *D*). These results suggest that DPI and rotenone initially inhibit angiogenesis, which, in turn, affects tumor growth, and that ROS production is required for tumor-induced angiogenesis and tumor growth.

DPI and rotenone inhibit the production of all three species of ROS: O_2^-, H_2O_2, and OH^- levels. To specifically test whether endogenous H_2O_2 is required for angiogenesis and tumor growth, OVCAR-3 cells were infected with adenovirus carrying GFP, catalase, or glutathione peroxidase (GPx), which specifically decreases H_2O_2 in the cells. These cells were used to analyze angiogenesis and tumor growth as described above. The infection of adenovirus carrying catalase or GPx abolished intracellular H_2O_2 production in the cells (Supplementary Fig. S3). Overexpression of catalase or GPx by adenovirus inhibited tumor-induced angiogenesis with 80% reduction of angiogenesis (Fig. 5*A* and *B*). This result suggests that H_2O_2 production in the ovarian cancer cells is required for tumor-induced angiogenesis. Catalase and GPx overexpression also greatly decreased tumor growth with 50% and 60% reduction of tumor weight, respectively (Fig. 5*C*). This result suggests that H_2O_2 production is required for ovarian tumor growth. In the tumor sections, high levels of VEGF and HIF-1α were expressed in the GFP control group and markedly decreased in those expressing catalase and GPx, which correlated with the inhibition of tumor-induced angiogenesis and tumor growth (Fig. 5*D*). Taken together, these results showed that ROS, especially H_2O_2 production in ovarian cancer cells, is required to induce angiogenesis and tumor growth and to increase VEGF and HIF-1α expression in the tumors.

To determine whether NOX4 expression regulates the expression of HIF-1 and VEGF and induction of angiogenesis, OVCAR-3 cells were transfected with NOX4 siRNA. NOX4 siRNA decreased the expression of NOX4 to the 30% level of the mock control (Fig. 6*A*). The levels of HIF-1α and VEGF expression were reduced to 50% of the control (Fig. 6*B* and *C*). To test the role of NOX4 in affecting angiogenesis, OVCAR-3 cells were transfected by NOX4 siRNA. The NOX4 siRNA treatment decreased tumor-induced angiogenesis more than 50% of the control (Fig. 6*D* and Supplementary Fig. S4). These results show that NOX4 expression is required in mediating HIF-1α and VEGF expression and in inducing angiogenesis.

Discussion

There are growing interests of ROS signaling in carcinogenesis. However, the direct roles and mechanism of ROS in tumor formation remain to be elucidated. In this study, we found that ovarian cancer cells spontaneously produced much higher levels of ROS than immortalized ovarian epithelial cells and observed that ROS may originate from the cytosolic NADPH oxidase and mitochondria in the cancer cells. We found that high levels of

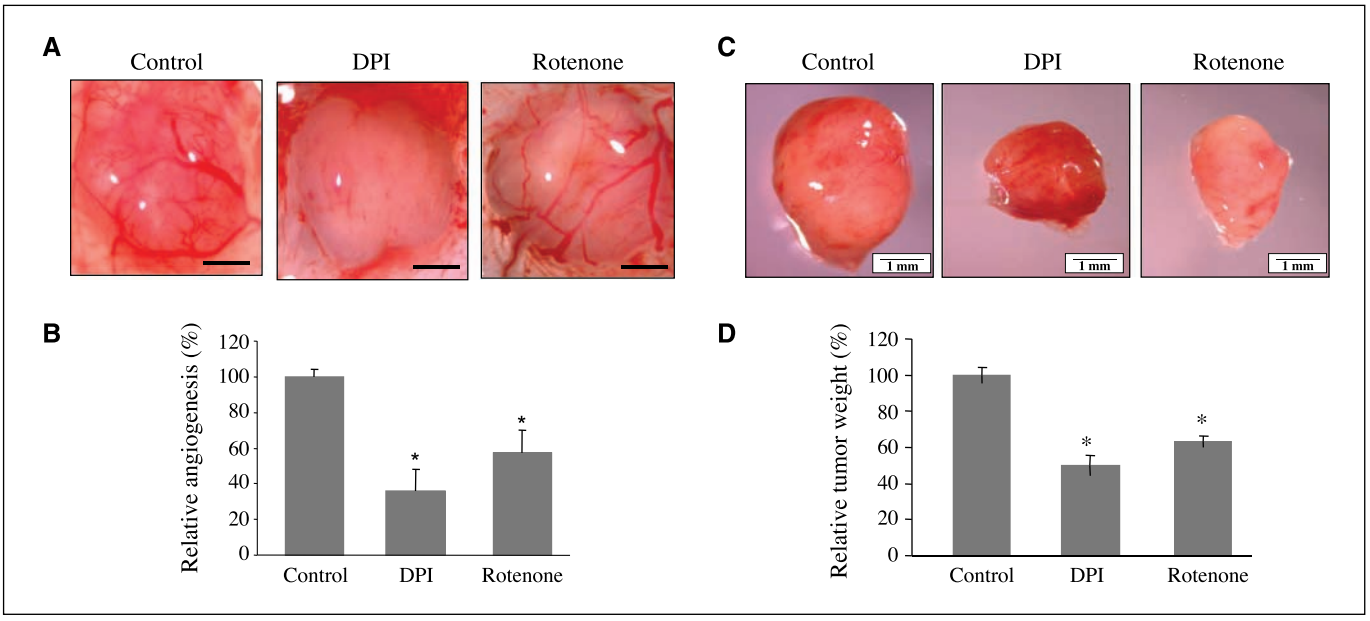

Figure 4. Inhibition of ROS by ROS inhibitors decreases angiogenesis and tumor growth *in vivo*. *A*, 2×10^6 ovarian cancer cells were mixed with Matrigel in the absence or presence of DPI (500 nmol/L) and rotenone (200 nmol/L) and implanted onto the chicken CAMs of 9-day-old chicken embryos. The Matrigel mixed with medium alone was used as a negative control. After the implantation for 4 d, the representative Matrigel plugs on the CAM were captured. *Bar*, 1 mm. *B*, blood vessels were counted on the CAM by counting the branching of blood vessels. The number of blood vessels as the index of angiogenesis was obtained from the CAMs of eight embryos per treatment. The data represent the mean ± SE of blood vessel number from replicate experiments, which was normalized to that of the control. *, $P < 0.05$, significant difference when the value of treatment was compared with that of the control. *C*, OVCAR-3 cells were treated with solvent, DPI (500 nmol/L), and rotenone (200 nmol/L); and implanted onto the CAMs. Tumor growth was analyzed 9 d after the implantation. Representative tumors are shown. *D*, relative tumor weight was the mean ± SE of tumor weight normalized to that of the control from eight different tumors.

ROS production are due to elevated NOX4 expression. It was reported that transforming growth factor-β1 up-regulated NOX4 expression and, thus, controlled the production of ROS (26, 27). In hepatocytes, it was through a NF-κB–dependent mechanism (28). We also observed that TGF-β1 inhibitor SB 431542 and NF-κB inhibitor PDTC significantly decreased NOX4 expression, indicating that TGF-β1/NF-κB pathway is involved in regulating NOX4 expression. High levels of ROS production were also observed in other human cancer cells including prostate cancer cells (Fig. 1*C*; refs. 29, 30). However, the biological role of ROS in cancer cells remains to be elucidated. Hypoxia-induced factor 1 (HIF-1) is a heterodimeric transcription factor composed of HIF-1α and HIF-1β subunits. HIF-1α, which is induced by hypoxia, growth factors, and oncogenes, plays a pivotal role in tumor growth and angiogenesis (31–33). In contrast, HIF-1β protein is constitutively expressed in human cells. Consistent with previous studies, hypoxia induced HIF-1α expression in OVCAR-3 and A2780 cells. Similarly, our previous study showed that high levels of HIF-1α were expressed in ovarian cancer cell lines A2780, A2780/CP70, and SKOV-3 (34). Here, we showed that ROS production in ovarian cancer cells was required for HIF-1α expression. To test what species of ROS were responsible for regulating HIF-1α expression, O_2^- scavenger SOD, H_2O_2 scavenger catalase, and OH^- scavenger sodium formate were used to treat the cells. SOD treatment increased the levels of HIF-1α expression, which may be due to the production of H_2O_2. Catalase inhibited HIF-1α expression in a dose-dependent manner and did not affect HIF-1β expression. The results indicated that H_2O_2 is responsible for mediating HIF-1α expression. To further test whether H_2O_2 is sufficient to induce the expression of HIF-1α, OVCAR-3 cells were treated with H_2O_2 at different times and doses. H_2O_2 enhanced HIF-1α level in a dose- and time-dependent manner, demonstrating that H_2O_2 is sufficient to increase HIF-1α expression.

VEGF is a potent inducer for angiogenesis and tumor growth (35, 36). The NADPH oxidase inhibitor DPI and the mitochondria complex I inhibitor rotenone inhibited VEGF protein level. They

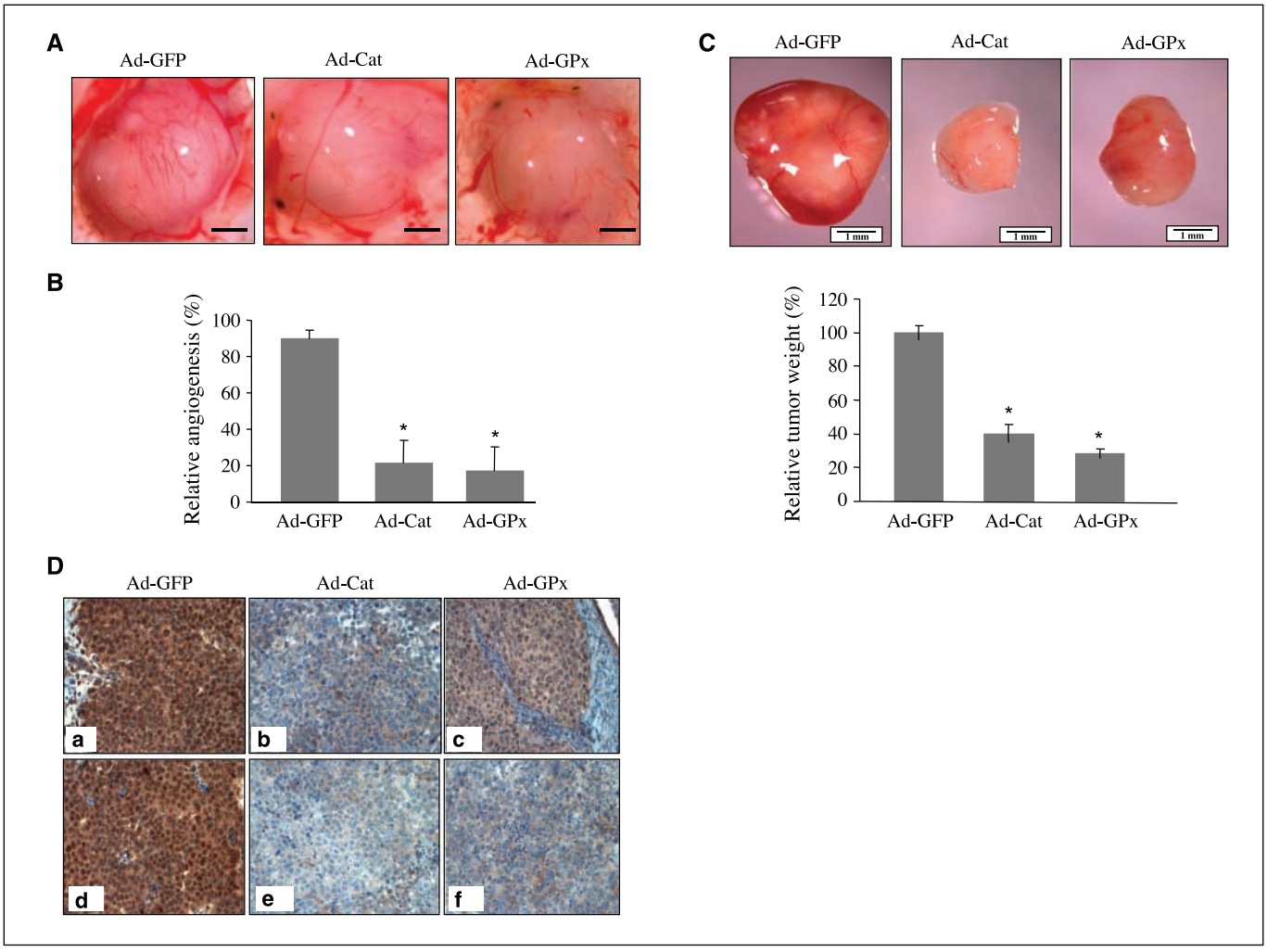

Figure 5. Inhibition of endogenous ROS by adenovirus carrying catalase or GPx decreased angiogenesis and tumor growth *in vivo*. *A,* ovarian cancer cells were infected by adenovirus carrying GFP, catalase, or GPx at 10 MOI for 24 h; then 2×10^6 cells were mixed with Matrigel and implanted onto the CAMs of 9-day-old chicken embryos as described above. The photos were the representative Matrigel plugs on the CAM. *Bar*, 1 mm. *B,* the relative number of blood vessels was quantified as above. *, $P < 0.05$, significant difference when the value of treatment was compared with that of the control. *C,* OVCAR-3 cells (2×10^6 cells) infected by adenovirus carrying GFP alone, catalase, or GPx at 10 MOI were implanted onto the CAMs. The photos showed the representative tumors from the CAM (*top*). Tumors were harvested and weighed 9 d after the implantation. Relative tumor weight was the mean ± SE of tumor weight normalized to that of the control from 8 to 10 different tumors (*bottom panel*). *D,* tumor sections were analyzed by immunohistochemistry analysis using antibodies against VEGF and HIF-1α. *a–c,* HIF-1α signals from the GFP control, catalase, and GPx treatment. *d–f,* VEGF signals from the GFP control, catalase, and GPx treatment.

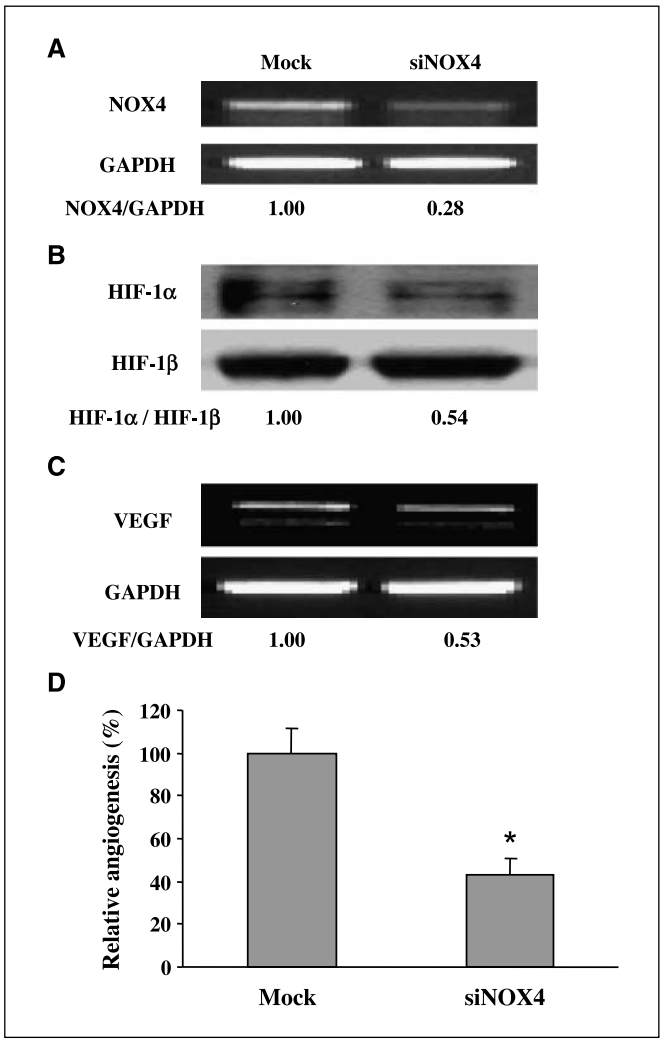

Figure 6. Inhibition of NOX4 expression by NOX4 siRNA decreased HIF-1α and VEGF expression and reduced angiogenesis. *A,* OVCAR-3 cells were transfected with 20 nmol/L NOX4 siRNA. The mRNA levels of NOX4 and GAPDH were determined by RT-PCR. *B,* cells were treated as above. Total protein lysates were extracted and subjected to immunoblotting analysis using antibodies against HIF-1α and HIF-1β. *C,* the mRNA levels of VEGF and GAPDH in the cells were determined by RT-PCR. *D,* OVCAR-3 cells were transfected with NOX4 siRNA. After 24 h, 2×10^6 cells were mixed with Matrigel and implanted onto the CAMs. The relative angiogenesis was analyzed on the CAM 4 d after the implantation and normalized to that of control from six replicate experiments. *, $P < 0.05$, significant difference when the value of siRNA treatment was compared with that of the control.

also decreased VEGF mRNA level and transcriptional activation, suggesting that ROS play an important role in regulating tumor-induced angiogenesis through controlling VEGF expression. The decrease of HIF-1α expression by ROS inhibitors inhibited VEGF transcriptional activation, suggesting that endogenous ROS regulate VEGF levels through HIF-1α expression. Angiogenesis is critical in tumor growth, invasion, and metastasis (18, 37–39). Although several evidences indicate that exogenous ROS induced by growth factors may increase neovascularization (4–6, 40, 41), the role of endogenous ROS in regulating angiogenesis and tumor growth remains to be elucidated. DPI and rotenone were found to inhibit neovascularization and tumor growth (Fig. 4), indicating that the inhibition of endogenous ROS decreased angiogenesis and tumor growth. To test the specific role of H_2O_2 in regulating angiogenesis and tumor growth, OVCAR-3 cells were infected with adenovirus-carrying catalase and GPx. The expression of catalase or GPx decreased intracellular ROS production and HIF-1α expression and significantly inhibited angiogenesis and tumor growth associated with the reduction of HIF-1α and VEGF expression (Fig. 5), showing that endogenous H_2O_2 was required for angiogenesis and tumor growth through the expression of HIF-1α and VEGF. These data suggest that endogenous ROS is very important for inducing angiogenesis and tumor development. Because we observed that NOX4 mediated ROS generation in OVCAR-3 cells, we further determined whether NOX4 is necessary in regulating HIF-1 and VEGF expression and in inducing angiogenesis. NOX4 siRNA greatly decreased NOX4 expression and HIF-1α and VEGF levels. NOX4 siRNA also significantly inhibited angiogenesis, suggesting that NOX4 is required for the induction of angiogenesis through ROS production (Fig. 6). NOX4 is required, but not sufficient for inducing VEGF transcriptional activation (Supplementary Fig. S5). Taken together, these results provide a new mechanism of high ROS production in ovarian cancer cells, show direct roles of ROS in regulating angiogenesis and tumor growth, and indicate that ROS may regulate tumor growth and angiogenesis through HIF-1α and VEGF expression.

Acknowledgments

Received 2/26/2007; revised 9/2/2007; accepted 9/13/2007.

Grant support: CA109460, RR016440, and CA123675 grants from the NIH; American Cancer Society Research Scholar Grant 04-076-01-TBE.

The costs of publication of this article were defrayed in part by the payment of page charges. This article must therefore be hereby marked *advertisement* in accordance with 18 U.S.C. Section 1734 solely to indicate this fact.

We thank Dr. Kathy Griendling (Emory University) for kindly providing the NOX4 plasmids.

References

1. Diplock AT, Rice-Evans CA, Burdon RH. Is there a significant role for lipid peroxidation in the causation of malignancy and for antioxidants in cancer prevention? Cancer Res 1994;54:1952–6s.
2. Kamata H, Hirata H. Redox regulation of cellular signalling. Cell Signal 1999;11:1–14.
3. Harfouche R, Malak NA, Brandes RP, Karsan A, Irani K, Hussain SN. Roles of reactive oxygen species in angiopoietin-1/tie-2 receptor signaling. FASEB J 2005; 19:1728–30.
4. Liu LZ, Hu XW, Xia C, et al. Reactive oxygen species regulate epidermal growth factor-induced vascular endothelial growth factor and hypoxia-inducible factor-1α expression through activation of AKT and P70S6K1 in human ovarian cancer cells. Free Radic Biol Med 2006;41:1521–33.
5. Zhou Q, Liu LZ, Fu B, et al. Reactive oxygen species regulate insulin-induced VEGF and HIF-1{α} expression through the activation of p70S6K1 in human prostate cancer cells. Carcinogenesis 2007;28:28–37.
6. Kim YM, Kim KE, Koh GY, Ho YS, Lee KJ. Hydrogen peroxide produced by angiopoietin-1 mediates angiogenesis. Cancer Res 2006;66:6167–74.
7. Jang M, Cai L, Udeani GO, et al. Cancer chemopreventive activity of resveratrol, a natural product derived from grapes. Science 1997;275:218–20.
8. Yang CS, Hong J, Hou Z, Sang S. Green tea polyphenols: antioxidative and prooxidative effects. J Nutr 2004;134:3181S.
9. Yang CS, Liao J, Yang GY, Lu G. Inhibition of lung tumorigenesis by tea. Exp Lung Res 2005;31: 135–44.
10. Singh RP, Agarwal R. Natural flavonoids targeting deregulated cell cycle progression in cancer cells. Curr Drug Targets 2006;7:345–54.
11. Bianchi NO, Bianchi MS, Richard SM. Mitochondrial genome instability in human cancers. Mutat Res 2001; 488:9–23.
12. Jackson AL, Loeb LA. The contribution of endogenous sources of DNA damage to the multiple mutations in cancer. Mutat Res 2001;477:7–21.
13. Puri PL, Avantaggiati ML, Burgio VL, et al. Reactive oxygen intermediates mediate angiotensin II-induced c-Jun.c-Fos heterodimer DNA binding activity and proliferative hypertrophic responses in myogenic cells. J Biol Chem 1995;270:22129–34.

14. Stevenson MA, Pollock SS, Coleman CN, Calderwood SK. X-irradiation, phorbol esters, and H_2O_2 stimulate mitogen-activated protein kinase activity in NIH-3T3 cells through the formation of reactive oxygen intermediates. Cancer Res 1994;54:12–5.
15. Schreck R, Meier B, Mannel DN, Droge W, Baeuerle PA. Dithiocarbamates as potent inhibitors of nuclear factor κB activation in intact cells. J Exp Med 1992;175: 1181–94.
16. Lee JM. Inhibition of p53-dependent apoptosis by the KIT tyrosine kinase: regulation of mitochondrial permeability transition and reactive oxygen species generation. Oncogene 1998;17:1653–62.
17. Guha M, Bai W, Nadler JL, Natarajan R. Molecular mechanisms of tumor necrosis factor α gene expression in monocytic cells via hyperglycemia-induced oxidant stress-dependent and -independent pathways. J Biol Chem 2000;275:17728–39.
18. Folkman J. Tumor angiogenesis: therapeutic implications. N Engl J Med 1971;285:1182–6.
19. Forsythe JA, Jiang BH, Iyer NV, et al. Activation of vascular endothelial growth factor gene transcription by hypoxia-inducible factor 1. Mol Cell Biol 1996;16: 4604–13.
20. Jiang BH, Rue E, Wang GL, Roe R, Semenza GL. Dimerization, DNA binding, and transactivation properties of hypoxia-inducible factor 1. J Biol Chem 1996; 271:17771–8.
21. Wang GL, Jiang BH, Rue EA, Semenza GL. Hypoxia-inducible factor 1 is a basic-helix-loop-helix-PAS heterodimer regulated by cellular O_2 tension. Proc Natl Acad Sci U S A 1995;92:5510–4.
22. Fang J, Xia C, Cao Z, Zheng JZ, Reed E, Jiang BH. Apigenin inhibits VEGF and HIF-1 expression via PI3K/AKT/p70S6K1 and HDM2/p53 pathways. FASEB J 2005; 19:342–53.
23. Ushio-Fukai M, Alexander RW. Reactive oxygen species as mediators of angiogenesis signaling: role of NAD(P)H oxidase. Mol Cell Biochem 2004;264:85–97.
24. Castier Y, Brandes RP, Leseche G, Tedgui A, Lehoux S. $p47^{phox}$-dependent NADPH oxidase regulates flow-induced vascular remodeling. Circ Res 2005;97:533–40.
25. Chowdhury AK, Watkins T, Parinandi NL, et al. Src-mediated tyrosine phosphorylation of $p47^{phox}$ in hyperoxia-induced activation of NADPH oxidase and generation of reactive oxygen species in lung endothelial cells. J Biol Chem 2005;280:20700–11.
26. Hu T, Ramachandrarao SP, Siva S, et al. Reactive oxygen species production via NADPH oxidase mediates TGF-β–induced cytoskeletal alterations in endothelial cells. Am J Physiol Renal Physiol 2005;289:F816–25.
27. Sturrock A, Cahill B, Norman K, et al. Transforming growth factor-β1 induces Nox4 NAD(P)H oxidase and reactive oxygen species-dependent proliferation in human pulmonary artery smooth muscle cells. Am J Physiol Lung Cell Mol Physiol 2006;290:L661–73.
28. Murillo MM, Carmona-Cuenca I, Del Castillo G, et al. Activation of NADPH oxidase by transforming growth factor-β (TGF-β) in hepatocytes mediates up-regulation of epidermal growth factor (EGF) receptor ligands through a NF-κB–dependent mechanism. Biochem J 2007;405:251–9.
29. Laurent A, Nicco C, Chereau C, et al. Controlling tumor growth by modulating endogenous production of reactive oxygen species. Cancer Res 2005;65:948–56.
30. Schoneich J. The induction of chromosomal aberrations by hydrogen peroxide in strains of ascites tumors in mice. Mutat Res 1967;4:384–8.
31. Jiang BH, Jiang G, Zheng JZ, Lu Z, Hunter T, Vogt PK. Phosphatidylinositol 3-kinase signaling controls levels of hypoxia-inducible factor 1. Cell Growth Differ 2001;12: 363–9.
32. Jiang BH, Agani F, Passaniti A, Semenza GL. V-SRC induces expression of hypoxia-inducible factor 1 (HIF-1) and transcription of genes encoding vascular endothelial growth factor and enolase 1: involvement of HIF-1 in tumor progression. Cancer Res 1997;57:5328–35.
33. Maxwell PH, Dachs GU, Gleadle JM, et al. Hypoxia-inducible factor-1 modulates gene expression in solid tumors and influences both angiogenesis and tumor growth. Proc Natl Acad Sci U S A 1997;94:8104–9.
34. Skinner HD, Zheng JZ, Fang J, Agani F, Jiang BH. Vascular endothelial growth factor transcriptional activation is mediated by hypoxia-inducible factor 1α, HDM2, and p70S6K1 in response to phosphatidylinositol 3-kinase/AKT signaling. J Biol Chem 2004;279: 45643–51.
35. Ferrara N. The role of VEGF in the regulation of physiological and pathological angiogenesis. EXS 2005; 94:209–31.
36. Coultas L, Chawengsaksophak K, Rossant J. Endothelial cells and VEGF in vascular development. Nature 2005;438:937–45.
37. Fidler IJ, Ellis LM. The implications of angiogenesis for the biology and therapy of cancer metastasis. Cell 1994;79:185–8.
38. Hanahan D. Signaling vascular morphogenesis and maintenance. Science 1997;277:48–50.
39. Risau W. Mechanisms of angiogenesis. Nature 1997; 386:671–4.
40. Lo YY, Cruz TF. Involvement of reactive oxygen species in cytokine and growth factor induction of c-fos expression in chondrocytes. J Biol Chem 1995;270: 11727–30.
41. Sattler M, Verma S, Shrikhande G, et al. The BCR/ABL tyrosine kinase induces production of reactive oxygen species in hematopoietic cells. J Biol Chem 2000; 275:24273–8.